

SOLAR RADIATION ESTIMATION ON BUILDING ROOFS AND WEB-BASED SOLAR CADASTRE

G. Aguiaro ^a, F. Nex ^a, F. Remondino ^a, R. De Filippi ^b, S. Droghetti ^b, C. Furlanello ^b

^a 3D Optical Metrology unit, Bruno Kessler Foundation, Trento, Italy
{aguiaro, franex, remondino}@fbk.eu, http://3dom.fbk.eu

^b Predictive Models for Biomedicine and Environment unit, Bruno Kessler Foundation, Trento, Italy
{defilippi, droghetti, furlan}@fbk.eu, http://mpba.fbk.eu

Commission II - WG7

KEY WORDS: Photovoltaic potential, DSM, Data integration, 3D modelling, WebGIS

ABSTRACT:

The aim of this study is the estimation of solar irradiance on building roofs in complex Alpine landscapes. Very high resolution geometric models of the building roofs are generated by means of advanced automated image matching methods. Models are combined with raster and vector data sources to estimate the incoming solar radiation hitting the roofs. The methodology takes into account for atmospheric effects, site latitude and elevation, slope and aspect of the terrain as well as the effects of shadows cast by surrounding buildings, chimneys, dormers, vegetation and terrain topography. An open source software solution has been developed and applied to a study area located in a mountainous site and containing some 1250 residential, commercial and industrial buildings. The method has been validated by data collected with a pyranometer and results made available through a prototype WebGIS platform.

1. INTRODUCTION

Solar technology is one of the possibilities for on-site clean energy production, as well as for the reduction of CO₂ emissions. Using photovoltaic (PV) panels, the incoming solar energy is transformed into electricity. The adoption of solar technologies is growing quickly, also thanks to large and urban-scale solar cadastre maps, often available on-line. Identifying suitable surfaces in urban or rural areas plays an important role both for the private investor and the public local community because PV systems need to be properly located and oriented in the environment to meet the required specifications (insolation time, surface orientation, panel type, characteristics of power network, etc.). In order to optimally exploit the advantages of solar technologies, it is crucial that predictive models provide reliable results. This is however a very complex task, because it requires huge amounts of sometimes missing or incomplete input data from different sources, ranging for example from meteorological data series to accurate geometric models of the buildings and the nearby terrain. Factors influencing a correct estimation of the incoming solar radiation include atmospheric conditions (e.g. air turbidity, cloudiness, aerosol, water vapour) and topography (e.g. shadowing by hills, mountains, nearby buildings, vegetation, etc.). In addition, conversion rates from solar radiation to electricity depend on the technology adopted for the PV panels (and all other devices like inverter, connecting wires, etc.). Today, common solar-module technologies are based on high-efficiency or standard crystalline silicon (c-Si), cadmium-telluride (CdTe), copper-indium-gallium-selenide (CIGS) or amorphous silicon (a-Si), with conversion efficiencies ranging from 20% down to 7% of the incoming solar radiation, respectively (Jacobson, 2009). This variability is due to the fact that solar panels generally never adsorb the whole spectrum of incoming radiation and so their characteristics must match the spectrum of available light.

Given the complexity of the whole sun-to-electricity pipeline, a multidisciplinary approach is required in order to correctly deal with the whole data process. However, existing literature deals mainly with specific aspects of the above-mentioned problems. As detailed and exhaustive list of references is beyond the scope

of this article, here only a selection of the most accepted and tested methodologies is mentioned. On-line solar cadastre (or solar GIS) services are already available at large scale, as in the case of SOLEMI [1] and SoDa [2], which provide solar irradiance maps up to global extents. When it comes to regional and urban applications, examples exist at different scales, like the PVGIS tool (Šúri et al., 2006) [3] or the city-wide solar cadastres of Berlin [4], Vienna [5], St. Gallen (Switzerland) [6] and Bressanone/Brixen (Italy) [7], just to name a few.

This study aims at defining and testing a pipeline implementing a web-based solar cadastre for building roofs (architectural scale) in Alpine areas, supporting PV energy production. The solution is intended to be used by municipalities for defining local policies and – in a simplified form – by the private end-user. A web-based tool has been introduced to provide an easy-to-understand and interactive answer to a quantitative estimation of eligibility of roofs for PV production. The goal is to encourage the wide-spread adoption of sustainable energy policies, both at public and at private level.

As case study, the area around the city of Trento (Italy) was selected (Fig. 1). For this area, the PV estimation system is currently available through PVGIS at 1 km ground resolution.

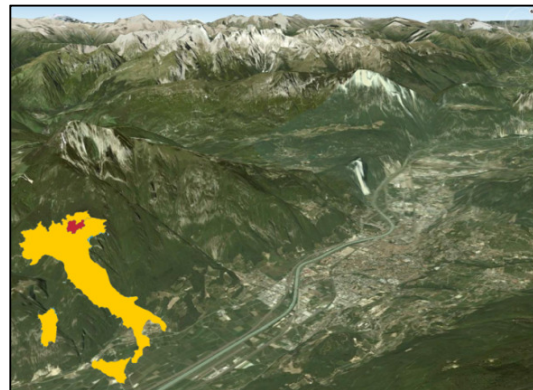


Figure 1: The city of Trento and the surrounding environs, in the North-East of Italy (image source: Google Earth).

This resolution does not support, however, precise and roof-based estimations. Here we propose a multi-scale solar irradiance estimation methodology, based on a combination of geometric 2D and 3D data and local atmospheric information.

The solar radiation estimation is computed within the free and open-source GRASS GIS environment. Although similar tools exist in other commercial and open-source GIS solutions (e.g. Esri ArcGIS and Saga GIS), the algorithms implemented in GRASS by Hofierka and Šúri (2002) in the *r.sun* module are well-known and tested in a variety of studies with reliable results (Kryza et al., 2010; Nguyen et al., 2009).

Obviously, the geometric resolution of the 3D models used to represent the buildings (or their roofs) plays an important role, as dormers or chimneys and their shadowing effects need to be considered. The need of geometric accuracy and the variety of scales to be considered – from architectural to regional – tend to be diverging forces, so that often a compromise has to be found. This is discussed in Aguiaro et al. (2011) where the pros and cons of using high-resolution roof models in an Alpine environment (i.e. where the direct shadowing effect by the surrounding mountains cannot be neglected) are reported. Following this work, this paper represents a direct continuation and extension, focussing mainly on these points:

- 1) Test of the developed methodology on a wider area;
- 2) Check of the available datasets not only regarding the study area, but with the purpose of extending the methodology to the whole province area (ca. 115×90 km),
- 3) Investigation of potential of automated image matching to achieve more detailed roof models at sub-metre resolution;
- 4) Finer analysis of atmospheric data series to better calibrate the *r.sun* model;
- 5) Development of a prototype WebGIS platform to publish the results and make them accessible to the public.

2. TEST AREA AND DATA SOURCES

The test area is located in Trento, a city of about 115.000 inhabitants in the Trentino-Alto Adige region (Northeast of Italy). It lies on the banks of the river Adige, in the homonymous valley and it is surrounded, mainly east and west, by the Alps, whereas the Adige valley stretches mainly north to south (Fig. 1). The test area is approximately 2.5×2.5 km wide, it contains circa 1250 residential, industrial and commercial buildings, with varying sizes and geometry complexity. Building location varies from the valley plane to the flanks of the Alps. Trento lies circa 200 m above sea level, however the nearby peaks, facing the city centre, are as high as 2100 m.

2.1 Data sources

Heterogeneous data were collected, at no additional costs, mainly from by the Autonomous Province of Trento (PAT) and Municipality of Trento. All spatial data, where applicable, were delivered already geo-referenced (WGS84/UTM32N) and consist of:

- A raster-based *DSM* (and the resulting *DTM*) derived from a LiDAR flight in 2006/7 at 1×1 m geometric resolution (or 2×2 m resolution for some scarcely inhabited mountainous areas). Height accuracy for the original LiDAR data is given as $\sigma_z=15$ cm for the *DSM*, and $\sigma_z=30$ cm for the *DTM*. Both *DSM* and *DTM* are provided as ESRI *ascii-grid* file.
- A set of 447 *cadastral maps* in vector format at nominal scale of 1:1000 available for the whole province and provided as *shapefiles*.
- A vector *topographic map*, at nominal scale of 1:10000, containing ca. 140000 building footprints and a rough classification of the building types (residential, religious,

commercial/industrial, etc.). Data are available for the whole province and provided as ESRI ArcGIS coverages.

- A set of 230 *digital orthophotos* produced in 2006 and 2009, with a ground sample distance (GSD) of 50 cm. Data are available for the whole province and provided as *tif* files.
- A block of 10 nadir *aerial images* acquired in 2009 with a RMKTOP15 analogic camera over the city of Trento (overlap of 60% along track and 30% across track). The digitised images have an average GSD of circa 12 cm.
- 20 *ground control points* (GCP), measured by the 3DOM unit in spring/summer 2011 in order to geo-reference the aerial images. The points were acquired by means of GNSS a receiver and post-processed using the Trento GNSS permanent station in order to achieve sub-decimetre accuracy.
- Average monthly values of the *air turbidity coefficients* (Linke data), provided as raster maps at 500 m resolution. Such data were obtained from the SoDa site [2] as a global dataset, then reprojected and resampled.
- *Solar radiation flux density* values (W/m^2) collected by a pyranometer located on the roof of an industrial building next to the study area. Flux density was sampled every 15 minutes during 7 years (2004-2010).

2.2 Data integration and storage

Due to the heterogeneity of the data sources, they were stored in a unique environment in order to facilitate data management and retrieval. The DBMS of choice was the free and open-source PostgreSQL 9.1 server, with its extension PostGIS (versions 1.5.3). Due to the presence of both vector and raster data, the beta version of upcoming PostGIS 2.0 was also tested, as it adds support for raster data, enabling a single set of SQL functions operating seamlessly on vector and raster data. Moreover, several raster formats can be imported by means of the GDAL library and saved either as internal or as file-system (out-db) rasters. Finally, PostgreSQL/PostGIS data layers can be easily accessed and published using GeoServer.

2.3 Vector and raster data analyses

All the *DSM* tiles were registered in PostgreSQL as ex-db rasters and a vector overview layer was created with all tiles' footprints. All building footprints from the cadastral and topographic vector maps were imported in two separate layers and checked against the *DSM* to decide which one to use in the successive steps. Availability of accurate footprints is indeed crucial, because they are used to easily identify the buildings and visualise the result in the WebGIS.

Both cadastral and topographic datasets have pros and cons, due to their origin and characteristics. The cadastral layer (Fig. 2a) generally contains building footprints represented at a higher level of detail and most footprints relate to single buildings, although they are not up-to-date as the reference time (2006/7, i.e. as of the LiDAR *DSM*). Several misalignments and distortions can be found, irregularly distributed, all over the dataset, when compared to the LiDAR *DSM*. A simple visual inspection suffices to detect planimetric displacements, sometimes as high as 10 m or more (Fig. 2c). The accompanying attribute data can be considered partially complete as some fields are missing data or are incorrectly assigned.

On the other hand, the topographic map contains footprints of groups of adjacent buildings, especially in the historical city centres (Fig. 2b), whereas newer areas (residential and commercial/industrial) are less aggregated.

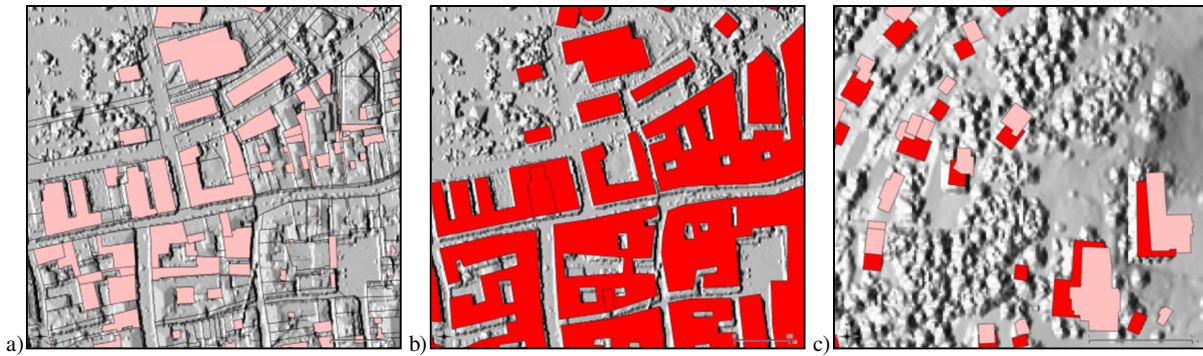


Figure 2: Evidence of issues with the vector maps of building footprints in the cadastral (a) and topographic (b) layers. The level of detail is higher in the former, but building footprints are not always correctly identified. The topographic layer is more complete but the buildings are grouped. Distortions and misalignments are particularly evident by overlapping the two layers (c).

The topographic dataset was digitised by three different companies starting from two distinct photogrammetric aerial surveys in 1998 and 2004, thus presents some mosaicking problems. Topographic footprints and DSM overlay correctly, are complete and up-to-date, with proper accompanying attribute.

For these reasons, the topographic layer was adopted as reference for all buildings' footprints. It must be noted that update and maintenance operations for both datasets are indeed hot topics themselves, both at regional and national level (Selvini, 2011), but they are beyond the scope of this work.

2.4 Processing of the aerial images over Trento

The available block of aerial images was used to extract a DSM at a higher, sub-metre resolution, in order to improve the geometric resolution of the building roofs and achieve a better estimation of the PV potential.

The extraction of precise and dense point clouds is nowadays possible by applying image matching techniques. Photogrammetric point clouds can indeed be considered comparable to LiDAR data especially in urban areas (Gehrke et al., 2010; Hirshmuller, 2008; Hiep et al., 2009). Point clouds generated from image matching can be much denser than typical LiDAR data and they allow a higher number of objects to be detected.

However, photogrammetric DSMs might be noisier than LiDAR acquisitions as they suffer from the image quality, the presence of shadows and object textures.

For the test area in Trento, the available aerial images (12 cm GSD) were processed with the open-source Apero/MicMac tools (Pierrot-Deseilligny and Clery, 2011; Paparoditis et al., 2006). Due to the low radiometric resolution of the images and the non-redundant overlap, the matching procedure delivered a DSM (point cloud with a regular step of about 24 cm) with some noisy areas close to the road sides and shadow areas. On the other hand the quality of the roof shapes reconstruction was only partially influenced. After the application of a median filter, a subsampled DSM at circa 50 cm resolution was generated (Fig. 3). This resolution was considered sufficient for the computation of the roof solar potentials.

In order to improve only the roof geometries of the test area and leave the remaining terrain and features unchanged, the photogrammetric DSM was intersected with the building footprints layer. Only cell values inside the footprints were kept and embedded into the oversampled LiDAR DSM. Furthermore, to check the quality of the extracted geometries, the height differences between the photogrammetric and LiDAR DSMs were computed (shown in Fig. 4). Major differences are found in case of chimneys/dormers or on roof-edges which are not represented or slightly smoothed in the LiDAR DSM (Fig. 5).

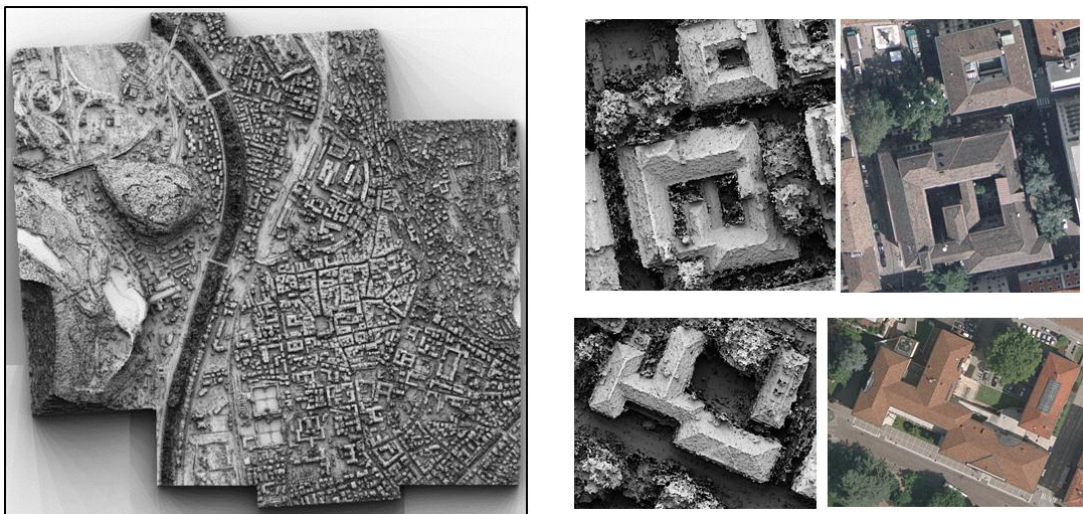


Figure 3: Shaded relief of the photogrammetric DSM (left). Details of the reconstructed roof geometries (right).

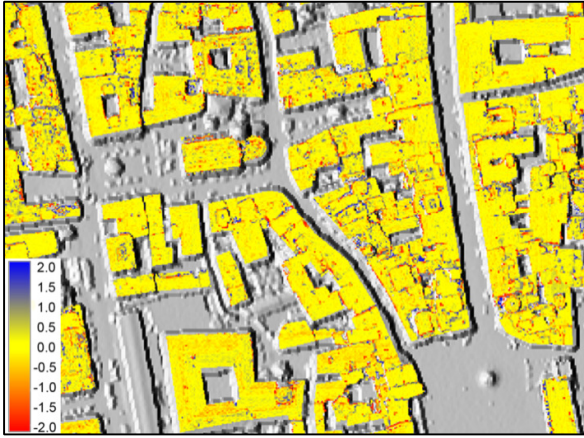


Figure 4: Difference map (in metres) between the LiDAR and photogrammetric DSMs (cell resolution: 0.5 m). A grey-coded shaded relief map of the DSM is shown as background for reference.

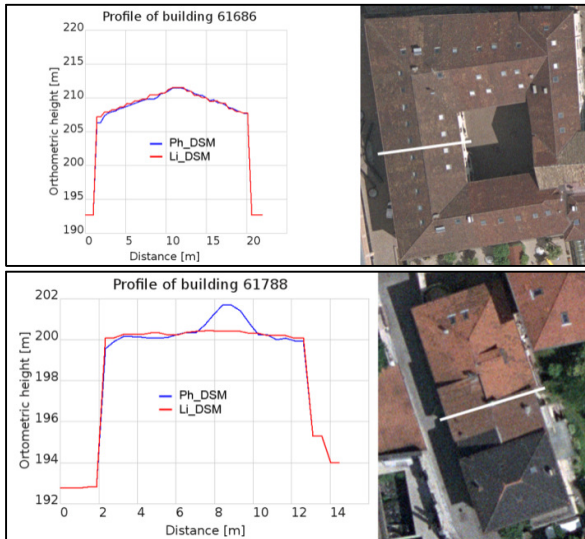


Figure 5: Profiles of two building roofs obtained from the photogrammetric (blue) and the LiDAR DSM (red). In case of flat roof faces [top], both models coincide. In case of irregular surfaces, the higher-resolution photogrammetric DSM can better describe the shape of a chimney.

3. ESTIMATION OF THE SOLAR RADIATION

3.1 Methodology workflow

Once all datasets were prepared and uploaded into the database, the actual solar irradiance computation began. As mentioned, GRASS GIS 6.4 was chosen as the working environment, because it is free and open-source and thanks to its convenient scripting capabilities (e.g. via Bash shell or Python). All computational work was carried out on a 1.6 GHz quad-core Core-i7 machine, with 8 GB of RAM and running a 64 bit version of Linux and GRASS GIS compiled at 64 bit to access all available RAM. The stepwise procedure will be described in the following.

Once the extents of the area to be analysed are defined, a spatial query is executed in PostgreSQL, having as result all DSM tiles covering the test area, plus all tiles needed to cover a buffer of 5 km around it. If not already available, all needed tiles are imported in GRASS and merged into a unique DSM.

Using a larger DSM than strictly needed allows to compute the horizon maps in such a way that adjacent mountains (and therefore their shadows) can be included directly in the model. Aspect and slope maps are calculated from the DSM. In an analogous way to the DSM, Linke air turbidity values are imported for the needed area.

In the next step, horizon maps are computed. With respect to the test area, computation extents are widened in order to take into account all surrounding cells in the DSM. The GRASS module `r.horizon` can be used to iteratively compute horizon maps for a given area, in that n maps are created for n directions: for each cell, the horizon height angle is stored for the given direction in a map. In this study, 24 non-overlapping horizon maps were computed at 15° intervals. Pre-computing horizon maps speeds up significantly solar irradiance estimation as only the relevant portion of DSM is considered in the iterations along time.

According to Šúri and Hofierka (2004), three main factors determine the interaction of the solar radiation with the Earth's atmosphere and surface: a) the position of the Earth with respect to the sun (thus the solar position above horizon), b) the terrain surface (i.e. the slope, the aspect and shadowing effects of the surrounding terrain features), c) the atmosphere, leading to a certain attenuation in terms of global radiation.

The GRASS `r.sun` module allows to model all above mentioned factors. The geometric factors (astronomic and terrestrial ones) can be modelled quite efficiently, while the atmospheric attenuation can be handled only within a certain level of accuracy. More specifically, `r.sun` computes direct, diffuse and ground reflected solar irradiance maps for a given day, latitude, surface and atmospheric conditions. Average monthly values of the air turbidity coefficients (Linke data) can be provided as a single value or as input raster maps: in this study the latter were used. The model computes radiation for the clear sky conditions, thus it does not take into consideration the spatial and temporal variation of clouds.

In total, 36 maps were obtained: for each month, direct, diffuse and global irradiance maps were calculated, yielding the average daily irradiance value (in Wh/m^2) for each month. The yearly average values were also calculated.

3.2 Calibration of r.sun

Data collected during a 7-year period of time (2004-2010) from a pyranometer located on the roof of an industrial building next to the study area were used to calibrate the global radiation model in `r.sun`. Solar radiation flux density values, sampled every 15 minutes by the pyranometer, were aggregated in order to obtain a series of 365 daily global radiation values (kWh/m^2).

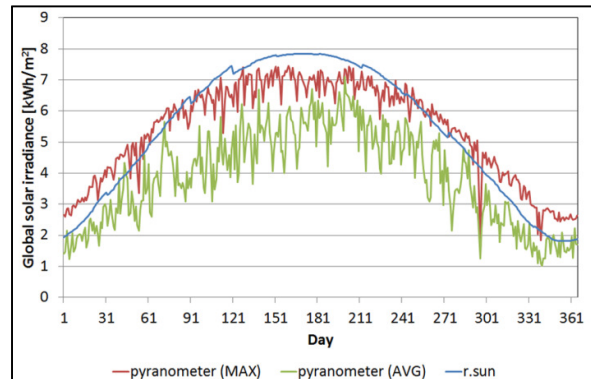


Figure 6: Daily values of maximum, average global irradiance flux (red and green, respectively) and `r.sun` global irradiance values (blue), at the pyranometer position.

Due to the fact that cloud cover information was not available, the daily maximum values over the 7-year-long observation interval were used as observed values for clear-sky solar radiation. In a similar way, average values were computed instead, in order to obtain a “standard” year which takes reduced solar radiation due to cloudiness into account. For comparison, 365 daily values, computed using r.sun at the same pyranometer position, were calculated. All three series of values are plotted in Fig. 6.

For clear sky conditions, r.sun tends to underestimate in winter and overestimate in summer, but on a year basis differences are negligible ($\approx 1\%$). With respect to the “standard” year, r.sun overestimates on a year basis by circa 39%.

From the 365 values, 12 monthly correction coefficients were computed, to be applied to the monthly radiation maps previously computed for the Trento area.

3.3 Identification of suitable roof areas and surface classification

Once the r.sun radiation maps were applied the correction coefficients, a reclassification was carried out on the map containing the average yearly values of global irradiance. Four classes, in increasing order of irradiance, were chosen to identify and distinguish areas on the roofs according to the amount of incoming radiation. They are:

- Class 0: cells with values of global irradiance below 0.9 kWh/m², considered unsuitable for PV-panels placement,
- Class 1: cells with values between 0.9 and 1.1 kWh/m²,
- Class 2: cells with values between 1.1 and 1.3 kWh/m²,
- Class 3: cells with values higher than 1.3 kWh/m², considered the best and most suitable areas on a roof.

The resulting reclassified raster map was pruned using the roof footprints and finally exported in the WebGIS.

3.4 Solar irradiance and roof models

The whole pipeline was repeated for the study area, using instead the higher-resolution roof models from the photogrammetric DSM. Monthly values of average daily direct, diffuse and global radiation were compared. Values were aggregated for all buildings and are plotted in Fig. 7.

Over the whole dataset, differences are negligible in absolute terms for the diffuse radiation. However, when it comes to the direct (and, thus, the global) radiation, the higher-resolution roof models deliver lower results during summer (up to -7.1% in June and July), while results are fairly comparable during the winter months. Differences can be due to the extra shadows cast for example by chimneys and dormers, not always present in the coarser LiDAR DSM at 1 m resolution. Noise due to possible

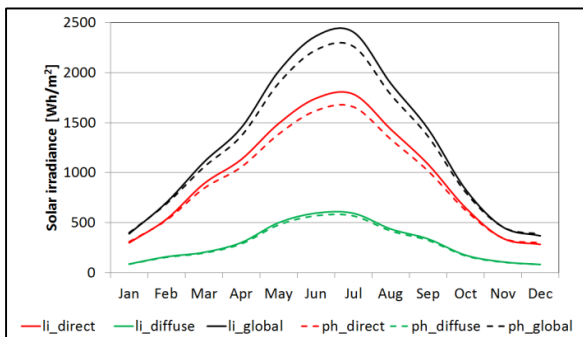


Figure 7: Average monthly values of daily irradiance (direct, diffuse and global), with the LiDAR DSM at 1 m (solid lines) and the photogrammetric DSM at 0.5 m (dashed lines).

poor image quality may also contribute to this reduction on roofs not perfectly modelled by the automatic image matching. On the other hand, using the results from the photogrammetric DSM assures to deliver “safer” results to the public, given the intrinsic approximations needed throughout the whole pipeline described in this work.

4. WEBGIS AND RESULTS PUBLICATION

Internet offers greater access to GIS services than traditional methods (Cobb and Olivero, 1997; Plewe, 1997), including planning. Open-access WebGIS-based planning services support structured cooperation and thus greater opportunities for sustainable solutions. Cost-effective access to baseline data is needed for effective planning (Peng, 1999): in the case of Trento, the challenge was to provide a user-friendly and versatile WebGIS solution for both decision-makers and private end-users.

The SolarWebGIS is a web platform with tools designed to map and extract descriptive statistics on building roofs potential for energy production using PV technologies. It is entirely built with open-source components, adopting the Open Geospatial Consortium (OGC) standards for geodata transmission and analysis, thus making the system completely interoperable with either proprietary and open-source systems.

The SolarWebGIS has a client-server structure based on the Django framework for the web-server architecture, the OpenGeo stack for mapping, and ExtJS for the client implementation. The current implementation, using data and results described in this paper, is available at <http://solarwebgis.fbk.eu>. An example is shown in Fig. 8 (left).

5. CONCLUSIONS AND OUTLOOK

The aim of this study was the estimation of solar radiation on building roofs in complex Alpine landscapes. Very high resolution geometric models of the building roofs are generated by means of advanced automated image matching methods. These data are used, in combination with other raster and vector data sources, to estimate the incoming solar radiation hitting the roofs. Atmospheric effects, geographical site position and elevation, terrain characteristics as well as shadowing by chimneys, dormers, nearby buildings, vegetation and terrain topography are taken into account. The methodology, validated with data collected with a pyranometer, delivered satisfactory results in the test area, which are now inserted into a prototype WebGIS platform for public access.

Existing data available from the municipality or other public sources were used to generate highly detailed roof models by advanced image matching algorithms. A solar cadastre of the building roofs was then developed to identify where and how much a roof is suitable for installing PV panels. The whole pipeline is based upon free and open-source software, from the generation of DSM and roof geometric models to GIS analyses, PV estimation, data repository, visualisation and publishing.

The workflow defined so far has allowed to improve data resolution and availability from 1 km to 50 cm resolution in the test area. Moreover, not only mutual shadowing by nearby objects or buildings, but also from surrounding orography can be included directly into the estimation model, because they can lead to non-negligible effects, especially in mountainous areas. Additionally, the web-based data publication tool enables also non-expert end-users to evaluate the suitability of their roofs for PV installations.

In summary, the adoption of free and open-source software has allowed a relatively smooth workflow and represents an attractive option for public administration willing to implement

this service at regional level (which is the next natural step of the presented work) in order to encourage wide-spread adoption of sustainable energy policies all over the province of Trento.

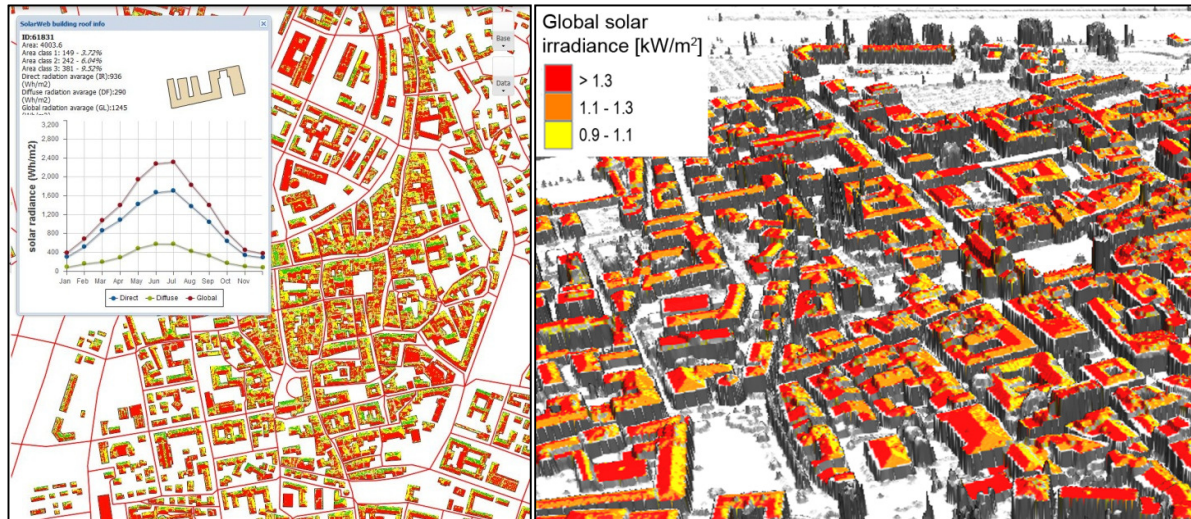


Figure 8: [Left] Screenshot from the WebGIS application with building footprints, the roofs classified according to the incoming global solar irradiance (yearly average values), and monthly statistics. [Right] 3D view of the study area showing the classified roofs mapped on top of the LiDAR DSM.

REFERENCES

- Aguilaro, G., Remondino, F., Stevanato, G., De Filippi, R., Furlanello, C., 2011: *Estimation of solar radiation on building roofs in mountainous areas*. IAPRS&SIS, Vol. 38(3/W22), pp. 155-160.
- Cobb, D.A., Olivero, A., 1997: *Online GIS service*. The Journal of Academic Librarianship, Vol. 1997/11, pp. 484-497.
- Gehrke, S., Morin, K., Downey, M., Boehrer, N., Fuchs, T., 2010: *Semi-global matching: an alternative to LiDAR for DSM generation?* IAPRS&SIS, Vol. 38(1), on CD-ROM.
- Hiep, V.H., Keriven, R., Labatut, P., Pons J.-P., 2009: *Towards high resolution multi-view stereo*. Proc. of Computer Vision and Pattern Recognition, pp. 1430-1437.
- Hirschmüller, H., 2008: *Stereo processing by semi-global matching and mutual information*. IEEE Transactions on Pattern Analysis and Machine Intelligence, Vol. 30(2), pp. 328-341.
- Hofierka, J., Šúri, M., 2002: *The solar radiation model for Open source GIS: implementation and applications*. Manuscript submitted to the International GRASS users conference in Trento, Italy.
- Jacobson, M.Z., 2009: *Review of solutions to global warming, air pollution and energy security*. Energy & Environmental Science, Vol. 2, pp. 148-173.
- Kryza, M., Szymanowski, M., Migala, K., et al., 2010: *Spatial information on total solar radiation: Application and evaluation of the r.sun model for the Wedel Jarlsberg Land, Svalbard*. Polish Polar Research, Vol. 31-1, pp. 17-32.
- Nguyen, H.T., Pearce, J.M., 2010: *Estimating potential photovoltaic yield with r.sun and the open source Geographical Resources Analysis Support System*. Solar Energy, Vol. 84(5), pp. 831-843.
- Papadoditis, N., Souchon, J.-P., Martinoty, G., Pierrot-Deseilligny, M., 2006: *High-end aerial digital cameras and their impact on the automation and quality of the production workflow*. ISPRS Journal of Photogrammetry and Remote Sensing, Vol. 60, pp. 400-412.
- Peng, Z.R., 1999: *An assessment framework for the development of Internet GIS*. Environment and Planning B: Planning and Design 26 (1), pp. 117-132.
- Pierrot-Deseilligny, M., Clery, I., 2011: *APER0, an open source bundle adjustment software for automatic calibration and orientation of set of images*. IAPRS&SIS, Vol. 38(5/W16), on CD-ROM.
- Plewe, B., 1997: *GIS Online: Information retrieval, mapping, and the Internet*. OnWord Press, Santa Fe, NM.
- Šúri, M., Hofierka, J., 2004: *A new GIS-based solar radiation model and its application to photovoltaic assessments*. Transactions in GIS, Vol. 8(2), pp. 175-190.
- Šúri, M., Huld, T., Dunlop, E.D., Albuissou, M., Wald, L., 2006: *Online data and tools for estimation of solar electricity in Africa: the PVGIS approach*. Proc. of the 21st European Photovoltaic Solar Energy Conference and Exhibition, Dresden, Germany.
- Selvini, A., 2011: *La banca dei dati Catastali: considerazioni sul rifacimento totale*. Geomedia, 3-2011, pp. 36-38.

REFERENCES FROM WEBSITES (16 Jan 2012)

- 01, <http://www.solemi.com>
- 02, <http://www.soda-is.com>
- 03, <http://re.jrc.ec.europa.eu/pvgis>
- 04, <http://www.businesslocationcenter.de/en/3d/A/i/1/seite0.jsp>
- 05, <http://www.wien.gv.at/umweltgut/public/>
- 06, <http://stadtplan.stadt.sg.ch>
- 07, <http://www.eurac.edu/it/research/institutes/renewableenergy/pvinitiativ/pvMap.html>

ACKNOWLEDGEMENTS

This work was partly supported by the ENERBUILD project (Alpine Space Program 11-2-1-AT), the ENVIROCHANGE project (PAT), the CIEM and 3M projects (co-founded Marie-Curie Actions FP7 – PCOFOUND – GA-2008-226070, acronym “Trentino Project”). The authors would also like to thank the Autonomous Province of Trento (PAT) and the Municipality of Trento, which kindly provided most of the employed spatial data, as well as Uniform for providing solar radiation data logged by its pyranometer, and Matteo Poletti of the MPBA research unit for technical support in validating the model.